Design and Modeling of a Periodic Single-Phase Sandwich Panel for Acoustic Insulation Applications

Chiara Gazzola [1], **Stefano Caverni** [1] **and Alberto Corigliano** [1,*]

[1] *Department of Civil and Environmental Engineering, Politecnico di Milano, Piazza Leonardo da Vinci, 32, 20133 Milano, Italy*

Correspondence*:
Corresponding Author
alberto.corigliano@polimi.it

ABSTRACT

Sandwich and composite panels are widely adopted in acoustic applications due to their sound insulation properties that overcome mass-law-based partitions in the medium-high frequency regions. A key aspect in the design procedure of acoustic panels is the control of the resonance dominated region of the Sound Transmission Loss (STL) curve. Within that frequency range such systems usually show acoustic weakness and poor insulation performances with respect to standard single layer solutions. In the present contribution we want to highlight an innovative approach for the sandwich partitions concept. A novel single-phase sandwich panel is realized adopting a periodic repetition of a properly designed unit cell. The resulting internal truss structure is self-sustained and its mechanical stiffness can be tuned to maximize the STL in the resonance dominated region. A series of parametric analysis is reported to show how the topology of the unit cell affects the noise reduction properties of the panel. An experimental validation is performed on a Nylon 3D printed prototype. The proposed panel is then integrated with some Locally Resonant elements that can be adopted to further improve the low frequency STL of the solution. Industrial and production considerations are also taken into account during the design process to make the solution industrially valid with a circular economy focus.

Keywords: sandwich panel; periodic panel; Sound Transmission Loss; circular economy

1 INTRODUCTION

The widespread adoption of sandwich-like acoustic panels in many sectors and applications is linked to their significant sound insulation performances combined with low weight and good mechanical strength. Mass-Air-Mass (MAM) and Mass-Spring-Mass (MSM) systems overcome single panel noise reduction performances over a wide frequency range. Multi-layered partitions are however characterized by a Mass-Spring-Mass resonance where clear weakness in terms of acoustic performances arise. For this reason such frequency range must be considered and rigorously analyzed during the design process. This resonance is strictly related to the stiffness of the multi-layered panel, which is determined by the geometry and material composition of the latter (C. W. Isaac and Wrona, 2020) (M. R. Zarastvand, 2021).

Different kind of cores for such panels have been investigated in the recent literature, including air cavities, porous or fibrous materials, honeycomb, truss or lattices structures. Honeycomb sandwiches are usually adopted in applications where high stiffness, good shock resistance and low mass is required. However, the latter features usually lead to an increase in the noise transmission through the structure (M. Radestock, 2019). Sandwich panels with truss-core demonstrate interesting dynamic, acoustic and mechanical properties that strongly depend on the core configuration (*e.g.* pyramids, tetrahedrons, hourglass) (Zhi-Hui Wen and Ma, 2021)(Dong-Wei Wang, 2017)(Zhen-Kun Guo and Tang, 2021).

The design process of the panel internal core is still a point of intense research (L. Quinteros and Ruiz, 2021) (C. Shen, 2013) (A. Spadoni, 2006). The main issue remains related to find an effective compromise between sound insulation performances and mechanical strength of the panel.

The aim of the present contribution is to propose a new sandwich panel concept with an engineered shape that match significant noise reduction performances and a structure with self-standing properties. The proposed innovative core is a modification of the one proposed in (C. Gazzola, 2021). It has been designed from the acoustic point of view to not overstiffen the panel and leave to the airgap the main stiffness contribution that defines the system resonance.

A series of parametric analysis has been carried out to optimize the acoustic performances of the sandwich panel in the resonance dominated region and to define the more promising configuration in terms of internal beam dimensions and presence of holes digged on the massive elements of the unit cell.

An additional aim of this work is to show further developments that can be implemented to improve the low frequency performances of the proposed panel with a Metamaterial based approach, coupling its core with Locally Resonant elements, similarly to the strategy proposed in (Filho et al., 2019) (de Melo Filho et al., 2019)(Lin et al., 2016) (de Melo Filho et al., 2020). Inclusions that act as Locally Resonant elements are introduced in the panel core, increasing the STL response in the 200-250 Hz region.

Another point taken into account in the design process is the industrialization of the panel through a circular economy approach. The panel core is conceived as a single-phase structure, which can be entirely produced through injection molding technique. This makes possible the realization of an acoustic insulating solution entirely made in regenerated plastic material.

The paper is structured as follows: the panel unit cell geometry and the numerical design approach are described in section 2. Results of numerical simulations and parametric analyses are reported in section 3 as well as the analytical lumped mass model to predict the MSM resonance frequency. In section 4 experimental results and validation of performances of the final selected design on a 3D printed panel are presented. In section 5 a Metamaterial approach for the panel is introduced from the numerical point of view. The proposed solution, *i.e.* the introduction of local resonators embedded in the unit cell, can be implemented to improve the STL response of the partition in critical parts of the spectrum at low frequencies. Finally, in section 6 conclusions are drawn.

2 MATERIALS AND METHODS

In this section a detailed description of the acoustic panel unit cell is presented along with the numerical tools exploited for the SPL estimation.

2.1 Acoustic Panel Geometry

The acoustic panel core is composed by a periodic structure with an in-plane repetition of a primitive cell.

The unit cell geometry is a modification of the one proposed in (C. Gazzola, 2021). The latter was composed by six massive pyramidal elements connected by a 3D frame and it was designed according to the principle of *separation of modes* (D'Alessandro et al., 2017) to obtain an ultrawide band gap at low frequencies (Fig. 1). This ensured that the mechanical modes of the core do not interfere with the acoustic transmission loss performances of the panel. The lumped parameter model proposed for this configuration showed the needed modifications in the geometry of the unit cell to optimize the STL performance at low frequencies. In particular, it was shown that the massive elements can be redistributed to maximize the lateral mass of the unit cell and minimize the internal one, which does not contribute to the modal mass of the MSM resonance mode. Moreover, the frame stiffness can be further reduced in order to make the mechanical stiffness negligible with respect to the air stiffness. These considerations have been taken into account to propose the innovative unit cell of this contribution.

The unit cell here analysed consists of two massive elements (Fig. 1a) connected by four elastic ligaments placed on a cross shaped frame that give structural stiffness to the panel (Fig. 1b). The aforementioned internal core is then integrated with a couple of 3.0 mm thick planar elements to create the final acoustic partition (Fig. 1d).

The working principle of the beam elements has been designed integrating the geometry proposed in (C. Gazzola, 2021) with industrial and production considerations for plastic injection molding. The flexural behaviour of the ligaments, from the dynamic and acoustic point of view, allows to play with an additional degree of freedom in the panel mechanical stiffness definition. At the same time, the panel can be conceived as a monolithic sandwich structure with both massive and ligament elements made of the same material, thus obtaining a suitable configuration for plastic molding manufacturing.

This type of production approach brings some additional constraints in the definition of the geometry of the unit cell *e.g.* undercuts must be avoided and holes are needed in the massive elements to facilitate the cooling process after the molding of the plastic. The unit cell has global dimensions of 60x60x46 mm. The fundamental geometrical features of the cell are highlighted in Fig. 2. In particular, $l_{mass} = 0.057\ m$, $b_{mass} = 0.016\ m$, $h_1 = h_2 = 0.0255\ m$, $l_{beam} = 0.026\ m$, $w_1 = 0.004\ m$, $w_2 = 0.002\ m$, $d = 0.008\ m$ and $a = 0.060\ m$. The material adopted for the prototype and for all the numerical simulations reported in what follows, is Nylon PA12, characterized by a Young's modulus E=1.586 GPa, Poisson's ratio ν=0.4, volumetric mass density ρ=1000 kg/m^3 and loss factor η=0.05. This lead to an overall partition mass of 26 kg/m^2.

2.2 Acoustic Panel Modeling

The Sound Transmission Loss (STL) of the proposed solution is determined numerically adopting a FEM plane wave model (Langfeldt and Gleine, 2019) implemented in COMSOL Multiphysics v5.6, by coupling the Pressure Acoustics and Structural Mechanics modules. As shown in Fig. 3, a primitive cell is modeled and the performances of the entire panel are reproduced due to the application of Bloch-Floquet boundary conditions, both at the lateral boundaries of the unit cell (see Fig. 3b) and at the air domain along the tube.

Perfectly matched layers (PML) are placed on the tube terminations.
The calculation of the STL is computed as:

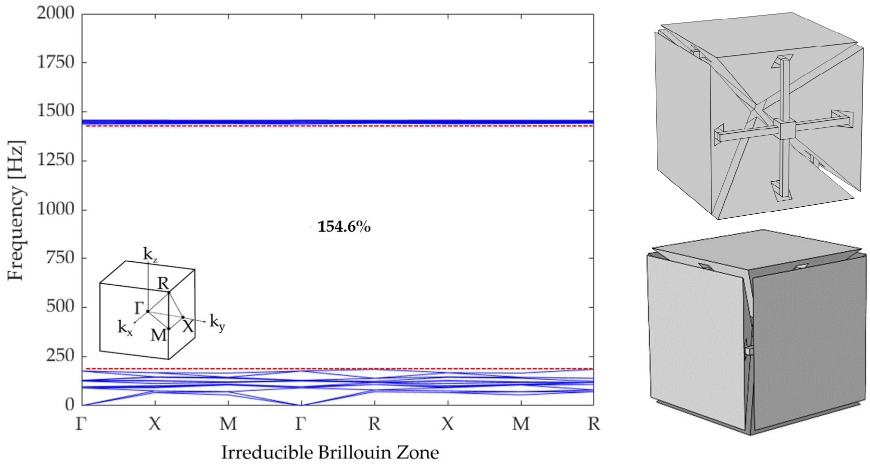

Figure 1. Dispersion diagram of the unit cell proposed in (C. Gazzola, 2021) with schematic of the investigated Irreducible Brillouin Zone. The red dotted lines identify the opening and closing frequencies of the first band gap, respectively, $f_o = 184$ Hz and $f_c = 1437$ Hz. The gap to mid-gap ratio is also reported.

$$STL = 20log_{10}\left(\frac{|P_{in}|}{|P_{out}|}\right), \tag{1}$$

with P_{in} and P_{out} representing the sound pressure computed at two sections before and after the sound insulation module. A normal incidence pressure wave model (without structural damping) is adopted for the simulations reported in section 3. In that section a lumped mass analytical model is presented with the aim of predicting the low frequency resonances by means of a simplified tool. In section 4, instead, the numerical STL is computed with a complete FEM model that takes into account both diffuse incidence equations and panel finite size correction, in order to have the best agreement between numerical and experimental data. The complete model formulation is here summarized:

$$STL_{diff,corr} = -10log_{10}\left(\frac{\int_0^{\theta_{lim}} |T(\theta)|^2\sigma_{R,avg}(\theta)\cos(\theta)^2\sin(\theta)d\theta}{\int_0^{\theta_{lim}}\cos(\theta)\sin(\theta)d\theta}\right) \tag{2}$$

being $T(\theta)$ the transmission coefficient, θ_{lim} = 90 deg and $\sigma_{R,avg}$ the averaged geometrical efficiency with its dependency on the incidence angle. Eight frequencies in each 1/3 octave band and twenty incidence angles between 0 and 89 degrees. A Standard Linear viscoelastic behavior is adopted in the FEM model which results are reported in section 4.

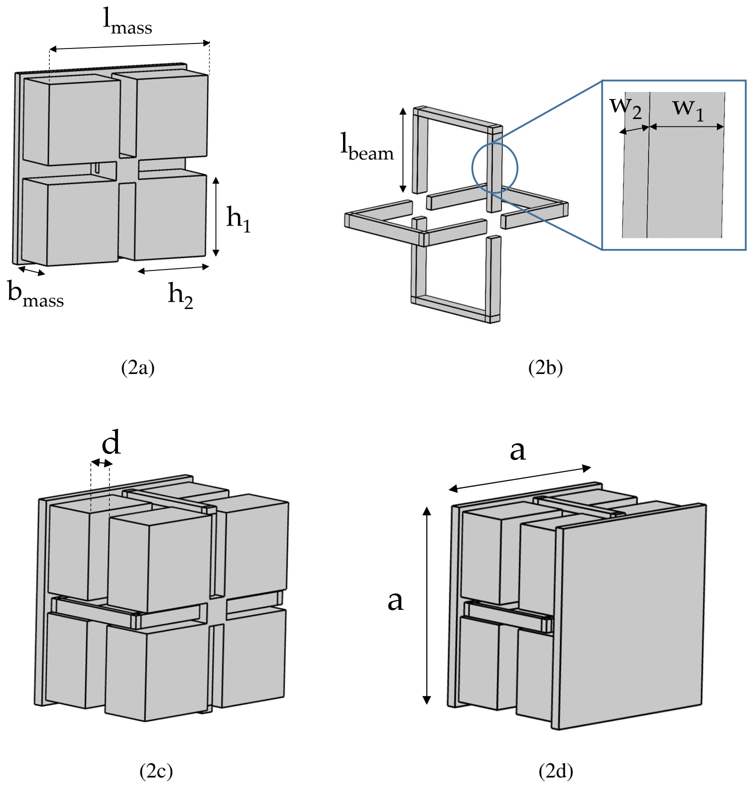

Figure 2. Unit cell geometry: (a) Massive elements connected by (b) four ligaments placed on a cross shaped frame. (c) Masses and internal frame assembly and (d) complete external view of the unit cell 60x60x46 mm.

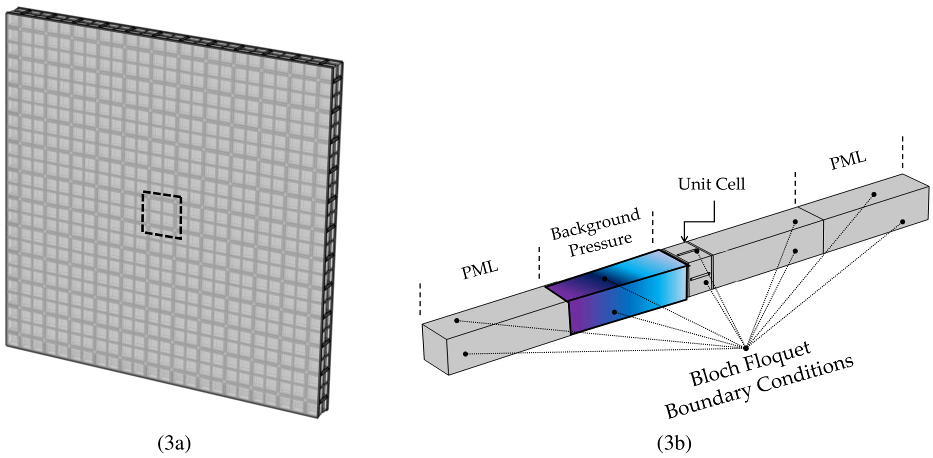

Figure 3. (a) Complete acoustic panel view and identification of the modeled unit cell. (b) Plane wave FEM model for sound transmission loss calculation.

The complete formulation of the constitutive law can be found in previous works (D'Alessandro et al., 2019)(D'Alessandro et al., 2016), while further details about the numerical formulation are reported in (C. Gazzola, 2021) and (Bonfiglio et al., 2016).

3 NUMERICAL RESULTS

In what follows, a set of parametric studies is presented, to show the panel acoustic performances at varying some geometrical features of the unit cell. In particular, the effects in terms of STL modifying the geometric dimensions of the elastic frame (subsection 3.1) and the number and position of holes in the massive element (subsection 3.2) are presented. These studies allow to select the most effective unit cell configuration, then exploited to build the prototype for the experimental validation. To limit the computational burden, these preliminary simulations are performed adopting a normal incidence model setting $\theta = 0$ in the formulation reported in subsection 2.2.

3.1 Geometric dimensions of the elastic ligament

One of the main geometrical features that characterize the acoustic partition performances is the beam elements dimension. The STL curves by varying the ligaments dimension w_2 (Fig. 2b) in the range 2.0-4.0 mm are reported in Fig.4. The effect of reducing the beams thickness is a progressive shift at low frequency of the MSM resonance. For w_2=2.0 mm the latter occurs at 187 Hz. At medium-high frequency (between 500 Hz and 2000 Hz), the analysis on the ligaments dimension show a variation of the second resonance frequency that arise due to the frame flexural mode as shown in Fig. 5. From the graph presented in Fig. 4 the green STL curve (w_1=4.0 mm and w_2=2.0 mm) is selected to proceed with further analysis on the panel geometry.

3.2 Number and positions of holes

As mentioned in subsection 2.1, the geometry of the panel is designed considering the adoption of injection printable recycled materials. For this purpose, the massive elements that compose the panel core need to be holed to facilitate the mass production with recycled plastic molding. This technique is adopted in the mold design phase to avoid strong temperature gradients that can lead to permanent deformations on the finite plastic component. The geometry of the panel is hence modified as depicted in Fig. 6. In the proposed holed configurations the thickness of the massive elements is adjusted to preserve the core mass of the unholed configuration. In all the three configurations, the air volume enclosed in the holes is the same to maintain constant the stiffness contribution related to

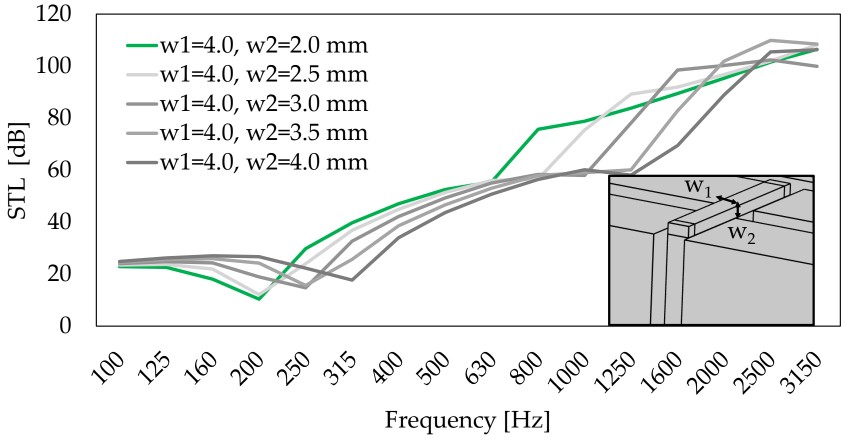

Figure 4. Sound Transmission Loss of the panel at varying beam dimensions.

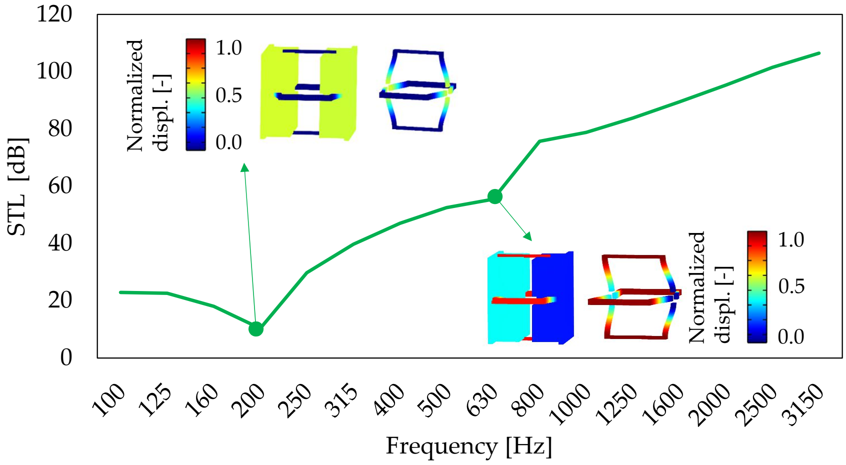

Figure 5. Sound Transmission Loss of the panel considering w_1=4.0 mm and w_2=2.0 mm with focus on the Mass-Spring-Mass resonance occurring at 187 Hz and beam elements mode at 630 Hz.

the air inside the partition.

This will be better highlighted in subsection 3.3.

Due to the equivalence in mass and stiffness, the STL curves for the three holed configurations are superimposed. The sixtyfour holes configuration is the one selected for the experimental validation due to a better voids distribution on the massive elements surfaces.

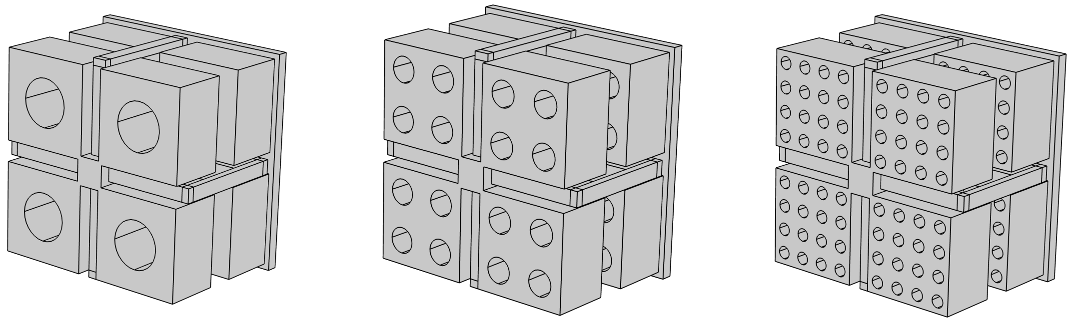

(6a) (6b) (6c)

Figure 6. Different holes configuration analyzed: (a) four holes configuration, (b) sixteen holes configuration, (c) sixtyfour holes configuration.

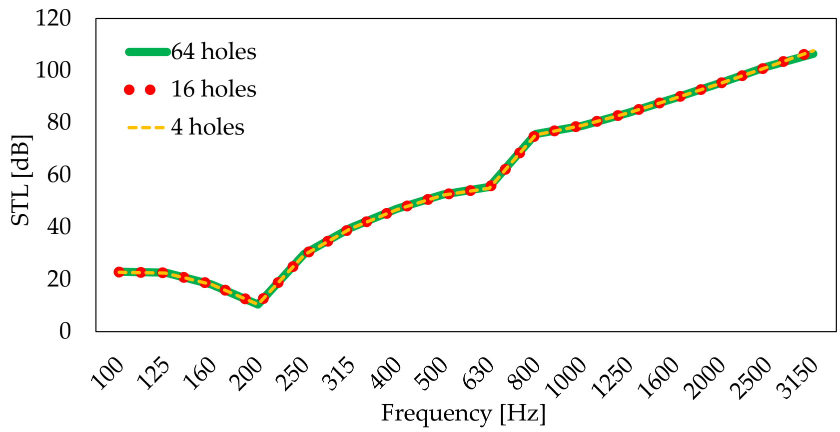

Figure 7. Sound Transmission Loss of the proposed acoustic partition at varying holes position and dimensions.

3.3 Lumped-parameter model

The Mass-Spring-Mass resonance frequency which appears at 187 Hz (Fig. 5) can be described by the lumped parameter model reported in Fig. 8a and following the procedure presented in (C. Gazzola, 2021). At this resonance the faceplates and the massive elements ($m_1 = m_2$=0.0042 kg) vibrate at the stiffness of the system, given by the air enclosed in the panel (k_a) and by the elastic ligament (k_m). The corresponding deformed shapes are reported in Fig. 8b for the lumped model and in Fig. 8c for the FEM model.

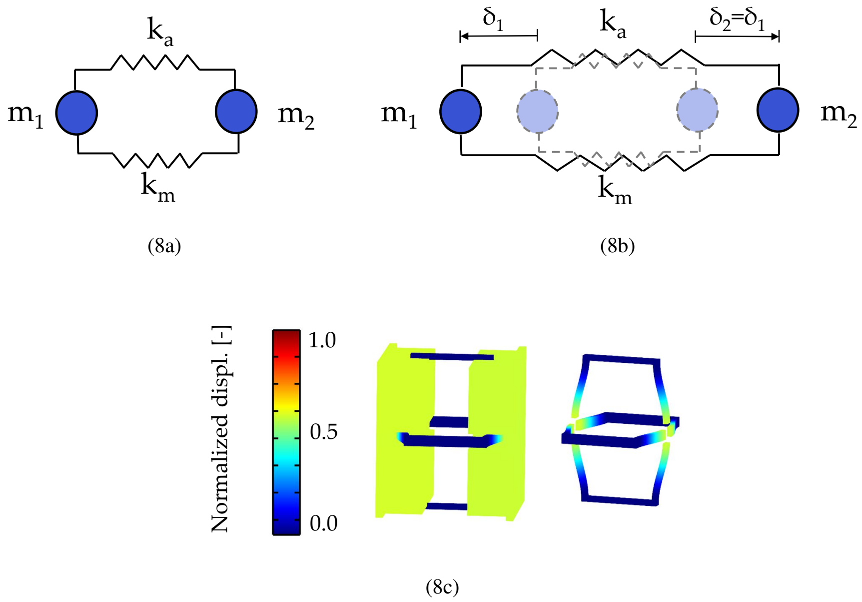

Figure 8. (a) Lumped-parameter model and (b) deformed shape corresponding to the Mass-Spring-Mass resonance at 187 Hz of the lumped model and (c) of the FEM model.

The air stiffness k_a is computed as $BA_p/d_{eq} = 24640$ N/m. $B = \rho_0 c^2$ represents the adiabatic bulk modulus of air, $\rho_0 = 1.225$ kg/m^3 and $c = 340$ m/s are the air density and the speed of sound considered. $A_p = 0.0036$ m^2 is the surface area of the unit cell and its equivalent thickness $d_{eq} = 20.7$ mm is derived computing the air volume enclosed in one unit cell (V_a=7.4484 $\cdot$ 10^{-5} m^3) and dividing it by the single unit cell surface (A_p).

The eight L shaped beams of the elastic frame determine the panel structural stiffness. In particular, the bending stiffness of the aforementioned ligaments is calculated considering a clamped-clamped beam scheme, whose bending stiffness reads $k_{m,1B} = 12EI/l^3 = 3248N/m$, with $I = 1/12 w_1^3 w_2$ and $l = l_{beam} - w_1/2$.

The mechanical stiffness of the four beams forming one half of the frame is equal to $k_g = 4 \cdot k_{m\,1B} = 12993$ N/m. Hence, the stiffness of the whole elastic structure is equal to $k_m = k_g/2 = 6496$ N/m, being the two grid in a series configuration.

According to D'Alambert's principle the lumped mass systems equation of motion are set:

$$\begin{cases} m_1\ddot{x}_1 + (k_a + k_m)x_1 - (k_a + k_m)x_2 = 0, & \text{for } m_1 \quad (3a) \\ m_2\ddot{x}_2 + (k_a + k_m)x_2 - (k_a + k_m)x_1 = 0, & \text{for } m_2 \quad (3b) \end{cases}$$

The harmonic motion hypothesis is considered introducing: $x = Xe^{i\omega t}$ to solve the linear eigenvalue problem. The MSM resonance predicted by the lumped model is equal to 189 Hz (+1$\%$ with respect to the FEM prediction).

The same frequency can be predicted starting from the MAM formula for a standard double-leaf partition, which reads (de Melo Filho et al., 2019; Norton and Karczub, 2010):

$$f_{MAM} = \frac{1}{2\pi}\sqrt{\frac{\rho_0 c^2}{d}\frac{m_1' + m_2'}{m_1' m_2'}}, \tag{4}$$

m_i' is the areal weight of the *i*-th wall leaf and d is the air-gap distance between the closing panels. Considering the definition of k_a, the aforementioned formula can be reinterpreted as:

$$f_{MAM} = \frac{1}{2\pi}\sqrt{k_a\frac{m_1 + m_2}{m_1 m_2}}, \tag{5}$$

with m_i the mass of the *i*-th wall leaf. For the panel under investigation there is also the stiffness contribution of the elastic frame, the MSM resonance can then be determined as:

$$f_{MAM} = \frac{1}{2\pi}\sqrt{(k_a + k_m)\frac{m_1 + m_2}{m_1 m_2}} = 189Hz. \tag{6}$$

It is worth mentioning that the mechanical stiffness represents only the 20% of the total stiffness.

4 EXPERIMENTAL RESULTS

In this section the final comparison between the tested 3D printed prototype and the complete numerical analysis of the panel is shown. The numerical STL curve is determined through the complete diffuse field FEM model presented in subsection 2.2 considering θ varying through twenty incidence angles between 0 and 90 degrees and eight frequencies for 1/3 octave band.

The experimental acoustic sound insulation of the panel is determined through a measurements campaign on a 3D printed prototype in Nylon PA12. The panel consists of 12x12x1 unit cells that result in a total dimension of 800x800x46 mm. A unit cell detailed view is depicted in Fig. 10c. Due to SLS 3D printing technology, the whole unit cell is printed together (front panel, back panel and core) avoiding the assembly procedure.

The panel prototype has been characterized in a coupled chambers laboratory (Fig. 10b) and the STL has been determined. Mastic sealing was arranged on the panel boundaries during the installation on the window between the reverberant and the hemi-anechoic chamber (see Fig. 10a). The total volume of the reverberant room is 252 m^3 and a tetrahedral source of the type Genelec 8351A is adopted. Six microphones $B\&K$ 1/4" type 4135 for sound pressure measurements in the source room are exploited, while the sound power in the receiving room is measured by means of a $B\&K$ sound intensity PP probe type 2681. The good agreement reached between the experimental test and the complete diffuse field model is shown in Fig. 9.

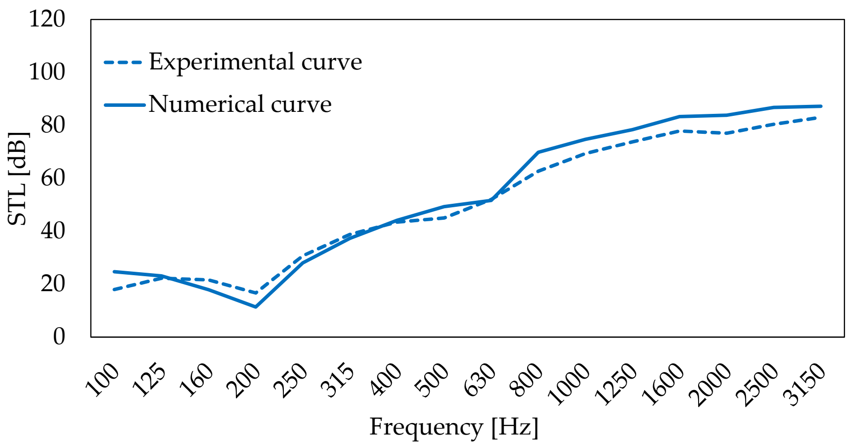

Figure 9. Comparison between the numerical STL curve determined through the diffuse field FEM model and experimental STL curve performed in double chamber lab.

5 METASOLUTION AND LOCALLY-RESONANT ELEMENTS

The purpose of this section is to give an idea of the potentiality that a single-phase sandwich partition can obtain in terms of transmission loss improvement if coupled with the metamaterial concept of locally resonant inclusions.

As mentioned in section 1, MSM panel show performances that exceed the sound insulation

(10a)

(10b)

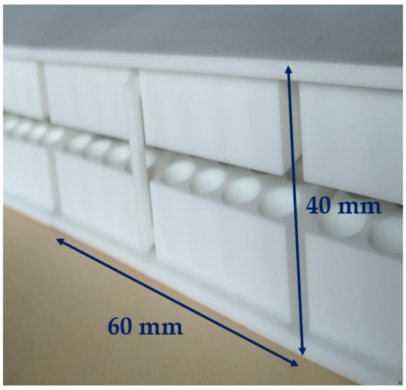

(10c)

Figure 10. (a) Acoustic panel mounted and sealed on test window, (b) reverberant room view (c) and prototype unit cell detail.

power of a common mass-law-based partition, especially in the medium-high frequency range. The resonance of the MSM system however results in a dip, in this case set to 187 Hz (Fig. 5), where the STL has its minimum value. For this reason, effective solutions based on locally resonant metamaterials principle to improve sandwich panels insulation at their resonance frequency are extensively present in recent literature (Filho et al., 2019) (de Melo Filho et al., 2019)(Lin et al., 2016) (de Melo Filho et al., 2020).
Coherently with the design process followed in the previous sections, a resonant element design embedded in the partition geometry is proposed. The massive elements that compose the panel core can be modified maintaining the injection moldable configuration, which is a key aspect for industrial production. The hosted resonant elements are hence designed by

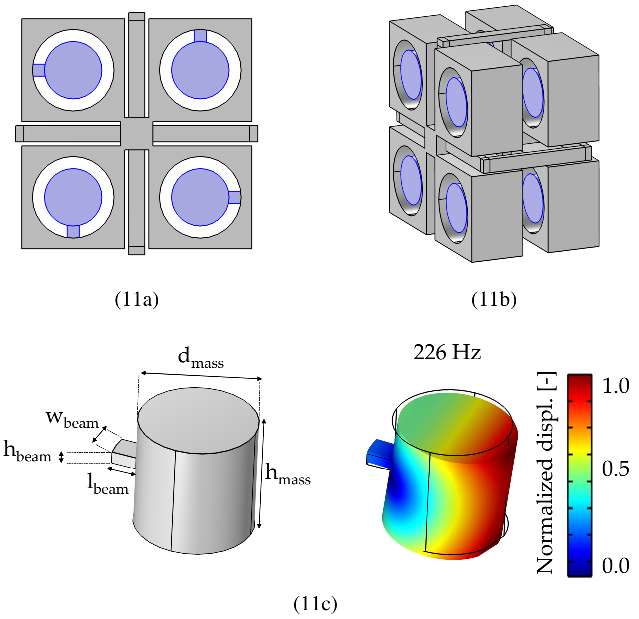

Figure 11. Unit Cell view of locally resonant hosting configuration. (a) Front view, (b) lateral view and (c) resonator geometry detail and first flexural eigenmode

tuning their own frequency with the one of the MSM system.
Resonators are composed of a beam element, linked to the main body of the unit cell, and a cylindrical massive part. The following dimensions are adopted, $d_{mass} = 0.014\ m$, $h_{mass} = 0.014\ m$, $l_{beam} = 0.003\ m$, $h_{beam} = 0.0015\ m$, $w_{beam} = 0.003\ m$ (see Fig. 11c).
The overall mass of the partition has been maintained to 26 kg/m^2 with the resonator mass set to 5 kg/m^2 ($m_{res}/M_{tot} = 19\%$).
Fig. 12 highlights the improvement in correspondence of the MSM dip of the baseline system due to the locally resonant element introduction. Right after the resonators frequency the sound transmission curve of the metamaterial panel converges towards the equivalent mass configuration.

6 CONCLUSIONS

The present contribution describes in detail the study, design, fabrication and experimental performances of an innovative acoustic sandwich panel. The peculiarity of the proposed geometry is the internal core, an in-plane repetition of multiple engineered unit cells,

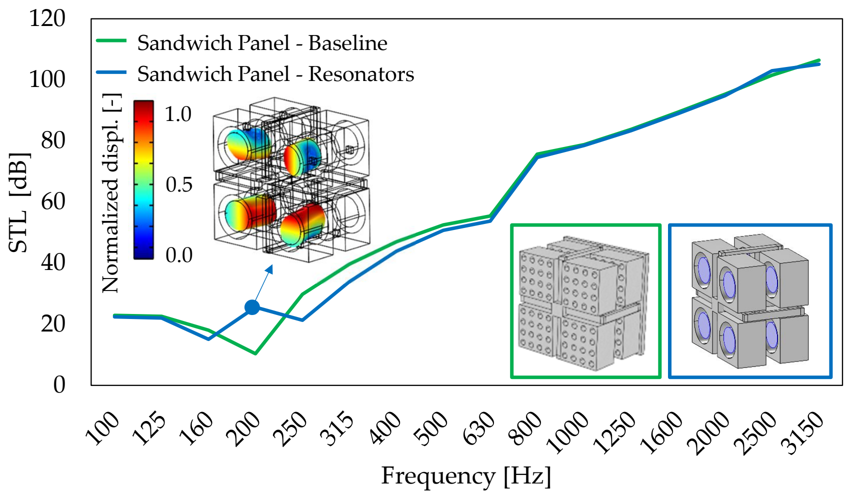

Figure 12. Normal incidence transmission loss comparison between baseline configuration and resonator hosting configuration.

coupled with two closing plane panels. The unit cell is composed by two principal massive elements supported by a frame of beams.

Such panel core is numerically and experimentally analyzed to give the partition a self-sustaining capability and optimized sound insulation performances.

In particular, the frame has been designed from the acoustic point of view to not overstiffen the panel and leave to the airgap the main stiffness contribution that defines the system MSM resonance, which is accurately predicted by the lumped parameter model proposed. During all the design process, considerations about the solution production via plastic injection molding have been take into account. The acoustic transmission loss performances are validated by an experimental campaign on a 3D-printed Nylon prototype, showing a good agreement between the proposed numerical impedance tube model and the sound insulation measured in double chamber lab. The last section introduces a further step in the optimization process of the panel explaining how the unit cell can be easily coupled with properly tuned locally resonant elements to improve the low frequency STL in correspondence of the MSM resonance. A more detailed investigation of this Metasolution will be the object of a future work.

CONFLICT OF INTEREST STATEMENT

The authors declare that the research was conducted in the absence of any commercial or financial relationships that could be construed as a potential conflict of interest.

AUTHOR CONTRIBUTIONS

Conceptualization, methodology and validation, C.G. and S.C.; writing—original draft preparation and figures preparation, C.G. and S.C.; writing—review and editing, S.C, C.G and A.C; supervision A.C; funding acquisition, A.C. All authors have read and agreed to the published version of the manuscript.

ACKNOWLEDGMENTS

The authors would like to thank Materiacustica S.r.l. and Paolo Bonfiglio for the precious support during the experimental tests.
The authors acknowledge the contribution of Fondazione Cariplo. The research has been carried out within the framework of Project ‘2018-1743 META-matErials as new teChnOlogy for high performing acoustic InSulatiOn paneLs, made of end of life MATerials’.

REFERENCES

A. Spadoni, M. R. (2006). Structural and acoustic behavior of chiral truss-core beams. *Journal of Vibration and Acoustics* 128, 625

Bonfiglio, P., Pompoli, F., and Lionti, R. (2016). A reduced-order integral formulation to account for the finite size effect of isotropic square panels using the transfer matrix method. *J Acoust Soc Am* 139. doi:10.1121/1.4945717

C. Gazzola, A. C., S. Caverni (2021). From mechanics to acoustics: Critical assessment of a robust metamaterial for acoustic insulation application. *Applied Acoustics* 183, 108311. doi:10.1016/j.apacoust.2021.108311

C. Shen, L. C. T. L., F.X. Xin (2013). Sound radiation of orthogonally stiffened laminated composite plates under airborne and structure borne excitations. *Composites Science and Technology* 84, 51–57. doi:10.1016/j.compscitech.2013.05.006

C. W. Isaac, M. P. and Wrona, S. (2020). Comparative study of sound transmission losses of sandwich composite double panelwalls. *Applied Sciences* 10, 1543. doi:doi: 10.3390/app10041543

D'Alessandro, L., Belloni, E., Ardito, R., Braghin, F., and Corigliano, A. (2017). Mechanical low-frequency filter via modes separation in 3d periodic structures. *Applied Physics Letters* 111, 231902. doi:10.1063/1.4995554

de Melo Filho, N., Claeys, C., Deckers, E., and Desmet, W. (2020). Metamaterial foam core sandwich panel designed to attenuate the mass-spring-mass resonance sound transmission loss dip. *Mechanical Systems and Signal Processing* 139, 106624. doi:10.1016/j.ymssp.2020.106624

de Melo Filho, N., Van Belle, L., Claeys, C., Deckers, E., and Desmet, W. (2019). Dynamic mass based sound transmission loss prediction of vibro-acoustic metamaterial double panels applied to the mass-air-mass resonance. *Journal of Sound and Vibration* 442, 28 – 44. doi:10.1016/j.jsv.2018.10.047

Dong-Wei Wang, L. M. (2017). Sound transmission through composite sandwich plate with pyramidal truss cores. *Composite Structures* 164, 104–117. doi:10.1016/j.compstruct.2016.11.088

D'Alessandro, L., Ardito, R., Braghin, F., and Corigliano, A. (2019). Low frequency 3d ultra-wide vibration attenuation via elastic metamaterial. *Scientific Reports* 9, 8039. doi:10.1038/s41598-019-44507-6

D'Alessandro, L., Belloni, E., Ardito, R., Corigliano, A., and Braghin, F. (2016). Modeling and experimental verification of an ultra-wide bandgap in 3d phononic crystal. *Applied Physics Letters* 109, 221907. doi:10.1063/1.4971290

Filho, D. M., Claeys, C., Deckers, E., and Desmet, W. (2019). Realisation of a thermoformed vibro-acoustic metamaterial for increased stl in acoustic resonance driven environments. *Applied Acoustics* 156, 78 – 82. doi:10.1016/j.apacoust.2019.07.007

L. Quinteros, E. L. C., V. Meruane and Ruiz, R. O. (2021). Phononic bandgap optimization in sandwich panels using cellular truss cores. *Materials* 14, 5236. doi:10.3390/ma14185236

Langfeldt, F. and Gleine, W. (2019). Membrane- and plate-type acoustic metamaterials with elastic unit cell edges. *Journal of Sound and Vibration* 453, 65 – 86. doi:10.1016/j.jsv.2019.04.018

Lin, Q., Lin, Q., Wang, Y., and Di, G. (2016). Sound insulation performance of sandwich structure compounded with a resonant acoustic metamaterial. *Composite Structures* 273, 114312. doi:10.1016/j.compstruct.2021.114312

M. R. Zarastvand, R. T., M. Ghassabi (2021). A review approach for sound propagation prediction of plate constructions. *Archives of Computational Methods in Engineering* 28, 2817–2843. doi:doi:10.1007/s11831-020-09482-6

M. Radestock, P. H. M., T. Haase (2019). Experimental transmission loss investigation of sandwich panels with different honeycomb core geometries. *Internoise*

Norton, M. P. and Karczub, D. G. (2010). *Fundamentals of Noise and Vibration Analysis for Engineers* (Cambridge University Press)

Zhen-Kun Guo, V. S. Y. Y., Guobiao Hu and Tang, L. (2021). Sound transmission through sandwich plate with hourglass lattice truss core. *Journal of Sandwich Structures and Materials* 23(6), 1902–1928. doi:10.1177/1099636220906819

Zhi-Hui Wen, D.-W. W. and Ma, L. (2021). Sound transmission loss of sandwich panel with closed octahedral core. *Journal of Sandwich Structures and Materials* 23(1), 174–193. doi:10.1177/1099636219829369